JOINT EUROPEAN TORUS

JET–P(89)34

G.T.A. Huysmans, R.M.O. Galvao, J.P. Goedbloed, E. Lazzaro,
P. Smeulders and JET Team

Ballooning Stability of JET Discharges

Ballooning Stability of JET Discharges

G.T.A. Huysmans[1], R.M.O. Galvao[2], J.P. Goedbloed[1], E. Lazzaro[3], P. Smeulders[3] and JET Team*

JET-Joint Undertaking, Culham Science Centre, OX14 3DB, Abingdon, UK

[1]FOM-Instituut voor Plasmafysica, Nieuwegein, The Netherlands
[2]Instituto e Pesquisas Espaciais, Sao José dos Campos, Brazil
[3]JET-Joint Undertaking, Culham Science Centre, OX14 3DB, Abingdon, UK
** See Appendix 1*

Preprint of Paper to be submitted for publication in
Plasma Physics and Controlled Fusion

BALLOONING STABILITY OF JET DISCHARGES

by

G.T.A. Huysmans*, R.M.O. Galvão**, J.P. Goedbloed*, E. Lazzaro P., Smeulders

JET Joint Undertaking, Abingdon, Oxon., OX14 3AE, UK
* FOM-Instituut voor Plasmafysica, Nieuwegein, The Netherlands
** Instituto de Pesquisas Espaciais, São José dos Campos, Brazil

Abstract

Conditions under which ballooning modes are expected to be excited have recently been obtained in two different types of discharges in JET. In the first type, extremely large pressure gradients have been produced in the plasma core through pellet injection in the current rise phase followed by strong additional heating. In the second type, the total pressure of the discharge is approaching the Troyon limit. The stability of these discharges with respect to the ideal MHD ballooning modes has been studied with the stability code HBT. The equilibria are reconstructed with the IDENTC code using the external magnetic measurements and the experimental pressure profile. The results show that the evaluated high beta discharge is unstable in the central region of the plasma. This instability is related to the low shear and not to a large pressure gradient, as expected at the Troyon limit. In the pellet discharges the regions with the large pressure gradients are unstable to ballooning modes at the time of the beta decay, which ends the period of enhanced performance. The maximum pressure gradient in these discharges is limited by the boundary of the first region of stability. The observed phenomena at the beta decay are similar to those observed at the beta limit in DIII-D and TFTR.

1. INTRODUCTION

The maximum beta values achieved in the various tokamaks are in reasonable agreement with the relationship $\beta_{max} = c\, I_p\,[MA] / B_0\,[T]\, a\,[m]$ of the Troyon-Sykes limit (TROYON et al., 1988). In the experiments, the value of c ranges from 2.0 to 2.8, whereas the numerically computed limiting value of c depends on the specific choice of the profiles but also falls in the relatively narrow range of 2.5 - 3.5.

There is also some agreement in the observed phenomena when beta is approaching the limiting value. In Doublet DIII-D (STRAIT et al. 1989) and ASDEX (GRUBER et al. 1986) this limit is seen as a disruptive limit at low q (< 3), as a saturation, or as a collapse of beta. In Doublet DIII-D a series of MHD modes is observed having mode numbers m/n = 5/4, 4/3, 3/2, 2/1 at resonance with increasing values of q. At the highest values of β, this either results in an m = 3, n = 2 mode causing a minor degradation of the confinement time by a factor of 10-20%, or the series stops with an m = 2, n = 1 mode which gives a much larger loss in confinement (a so-called β-collapse) or a disruption. The theoretical MHD stability analysis of these discharges predicts stability of the low-n modes, but marginal stability or even instability of high-n ideal ballooning modes in the central region and the edge of the plasma. In ASDEX, the toroidal mode number observed at the β limit is always n = 1, whereas the poloidal mode number m = 1, 3. At some times during the beta decay strong m = 2 and m = 3 activity is observed. Fishbones with m = 6 are also seen. Comparison with stability calculations suggests that the observed modes are pressure driven tearing modes (GRUBER et al. 1986). The discharges at the beta limit are stable to high-n ballooning modes, but resistive ballooning modes may become unstable (BECKER et al. 1987).

In TFTR (MC GUIRE et al. 1988), the disruptions at the beta limit occur at the higher values of q. Again, in the discharges that do not end in a disruption, MHD modes with mode numbers m/n = 3/2 (and less often 2/1) are observed causing a decrease in beta. These modes may also be seen by the flattening of the temperature and density profiles at the rational q value. [This is also seen in DIII-D]. At lower q ($q_{cyl} < 6$), the dominant mode numbers are m/n = 1/1. Although the signatures of the beta limit in TFTR are comparable with those of Doublet DIII-D, the scaling of β does not follow the Troyon scaling at higher q. Instead, β_{max} drops with q_{cyl} and the limit on beta seems to be set by a limit on the poloidal beta. However, the observed β limit is still in agreement with the MHD stability boundaries of the low-n kink and ideal ballooning modes. This difference is caused by the relatively peaked pressure profiles of the

TFTR supershots, whereas the Troyon limit is found after an optimization of the profiles which leads to relatively broad pressure profiles.

The fact that equilibria with a peaked pressure profile have a substantially lower β limit than equilibria with a broad pressure profile (HENDER et al. 1987) led us to the investigation of the ballooning stability of the pellet fuelled discharges of JET. In these discharges very strongly peaked pressure profiles are produced by pellet injection, followed by strong additional heating (JET TEAM 1988). The results of the stability analysis and a comparison with the experimental data are presented in Sec. 2.

In Sec. 3 we also discuss a second type of discharges, viz. the discharges with low plasma current and low toroidal field combined with strong ICRH heating which were an attempt to reach the β limit in JET.

Conclusions are drawn in Sec. 4.

2. DISCHARGES WITH PELLET FUELLING

In JET, limiter discharges with an enhanced performance are obtained by injection of a pellet in the current rise phase, followed by strong additional heating (JET TEAM 1988). These discharges are characterized by large pressure gradients ($dP/dr > 300$ kPa/m) in the central region of the plasma.

In this section we will analyse shot #17749. The time traces of the plasma current I_p, the total power, and the poloidal beta β_I are shown in Fig. 1. Also shown is the trace of β_I of a reference shot with approximately the same parameters and heating power, but with no pellet injected (shot #17747). In shot #17749, the pellet is injected at $t = 43.0$ sec. The value of β saturates at $\beta_I = 0.4$ and, subsequently, starts to drop at $t = 44.25$ sec, although the total heating power is constant. This drop is preceded by a sharp increase in the $n = 2$ activity accompanied by an increase in the $n = 4$ and a smaller increase of the $n = 3$ signal, while there is no significant change in the $n = 1$ activity (see Fig.2). Analysis of the soft x-ray emission indicates a poloidal mode number of $m = 3$. This $m/n = 3/2$ mode can also be seen as a flattened region around the $q = 1.5$ surface in the x-ray emissivity (see fig.3). The occurrence of this mode in JET discharges was shown to be related to a loss of confinement (SNIPES et al. 1988). Comparison of the MHD activity of the shots with and without pellet injection shows that the MHD activity starting at the onset of the ICRH heating is not related to the pellet injection.

The equilibrium needed for the stability analysis was calculated by means of the IDENTC code (BLUM et al. 1986, LAZZARO and MANTICA 1988) which fits the external magnetic

measurements and the experimental pressure profile to the calculated equilibrium. The electron pressure profile measured by the LIDAR diagnostic (SALZMANN et al. 1987) at the time of the increase of the n = 2 activity is shown in Fig. 4. Also shown is the electron pressure profile of the reference shot. The value for q on axis is 1.2 ± 0.2 as determined by both polarimetry (O'ROURKE et al. 1988) and IDENTC. The safety factor at the edge is 3.8 for the discharge with pellet and 4.1 for the discharge without pellet.

The equilibria reconstructed with IDENTC were analyzed with respect to ideal ballooning modes by means of the HBT code (GOEDBLOED et al. 1987). The results are shown in the shear versus pressure gradient diagram of Fig.5a [a so-called s-α diagram, where $s \equiv 2(\psi/q)(dq/d\psi)$, and $\alpha \equiv -(4q^{*2}/\varepsilon B^2)\sqrt{\psi}\, dp/d\psi$]. Only the central part of the plasma $(0 < \psi < 0.3)$ is shown. The stability boundary of the first region of stability (the left side of the shaded area in Fig. 5a) is determined by increasing the total pressure, while keeping the shape of the pressure profile fixed in a flux-conserving sequence. It turns out that the largest pressure gradients (in the range $0.06 < \psi < 0.16$) of the pellet shot cause instability with respect to high-n ballooning modes, with a growth rate of about $2.5 \times 10^{-2}\, \tau_A^{-1}$ sec. The reference shot, on the other hand, is far from instability. In order to account for the uncertainty of the experimental value for q on axis, the ballooning stability was calculated for different values of q_0. The value of q_0 was changed by changing the peaking of the diamagnetic profile, while keeping the pressure profile fixed. Although the unstable region becomes smaller with increasing q_0, the largest pressure gradients are unstable up to $q_0 \approx 1.5$.

An estimate of the toroidal mode number that is marginally stable with respect to ballooning modes can be calculated from the first order correction of the $n^{-1/2}$ expansion (CONNOR et al. 1984). This gives the growth rate as a function of the toroidal mode number :

$$\omega^2 = \omega_0^2 + ((\partial^2\omega^2/\partial\psi^2)(\partial^2\omega^2/\partial\theta_0^2))^{1/2} / (2n\nu'), \qquad (1)$$

where ν' is the local shear and θ_0 is the integration constant related to the radial wave vector. In this case, the mode number with zero growth rate turns out to be $n_c \approx 7$ (see fig 5b). This indicates that finite Larmor radius effects are not likely to stabilize the mode.

A correlation between violation of the ballooning stability and the occurrence of an internal disruption, which leads to a loss of energy and particle content, is also found in the ASDEX pellet shots with improved confinement (KAUFMANN et al. 1988).

The same equilibria have also been investigated with respect to stability of internal modes with low poloidal mode number, using the exact equilibria but employing the high-beta tokamak ordering in the stability analysis. The non-pellet discharge was found to be stable, whereas the peaked profile of the pellet shot is predicted to become unstable, but only for values of $\beta_l > 0.7$ and $q_0 \approx 1.0$.

Although the obtained β in the pellet case is only 40% of the Troyon limit and only a small part of the plasma volume is ballooning unstable to ideal ballooning modes, the observed phenomena are quite similar to those observed at the β limit in DIII-D and TFTR: violation of the ballooning stability is followed by m/n = 3/2 mode activity, accompanied by an increase in higher n mode activity. Possibly, the m/n = 3/2 mode is initiated by a broadening of the pressure and current density profile (increasing the local gradients) due to the ballooning instability, similar to that proposed for DIII-D as an explanation of the β collapse (STRAIT et al. 1988).

Higher pressure gradients could be obtained by raising the value of q on axis by broadening the current density profile. Access to the second region of stability would also require a lower shear at the position of the large gradients (TROYON et al. 1988).

3. HIGH BETA DISCHARGES

A series of discharges at low plasma current and low toroidal field (I_p = 1.5 MA, B_T = 1.5 T) with strong ICRH heating have been produced in JET in an attempt to reach the beta limit. The time traces of the total current, the heating power, and the central temperature of the discharge #14729 are shown in Fig. 6. In this discharge, one of the highest values of the ratio β/β_c was obtained, viz. β/β_c = 0.6. Also shown is the magnetic activity with mode numbers n = 1 and n = 3. We note that after t = 47 sec, the central electron cyclotron emission starts to show spikes superimposed on the usual sawteeth. These spikes are well correlated with the MHD activity as measured by the external coils. Furthermore, the activity after 47.5 sec seems to increase for larger mode numbers.

To investigate the possible role of ballooning modes, we have carried out a stability analysis at t = 48.0 sec, since the electron pressure profile measured by the lidar diagnostic was available for that time. In Fig. 7, the pressure profile obtained from a fit of the equilibrium to the magnetic measurements by the IDENTC code is compared with the measured pressure profile. In the stability analysis we use the more globally reconstructed profile in order to avoid possible ballooning instabilities caused by local disturbances of the pressure profile. The magnitude of the total pressure is determined by the value of the poloidal beta. The results of the high-n ballooning analysis are shown in the form of the s-α diagram of Fig. 8a. The plasma is found unstable in the central region indicated. It should be noted though that the cause of this instability is not the large pressure gradient associated with a high beta discharge, but the lack of shear in the center and the low value of q on axis (q_0 = 0.81). The low shear is also reflected in the shape of the eigenfunction (Fig. 8b). In the low shear central region, the standard

ballooning approximation is only valid when $(\psi dq/d\psi)^{-2} < n$ (HASTIE et al. 1981), which restricts the validity of the analysis to $n > 250$ for this case. Extrapolation of the growth rate to lower modenumbers, using Eq. (1), is then not possible because in the unstable low shear region $\omega^2(n^{-1})$ is expected to have an oscillatory behavior. This is related to the passage of rational values of nq through the most unstable flux surface (HASTIE et al. 1981, MANICKAM et al. 1987). However, this does not imply stability of the intermediate values of n. Infernal modes, which can be unstable even if ballooning are stable, may play a role here.

Finally, it should be noted that the unstable region is localized within the q = 1 surface, so that a possible consequence of the instability might be to trigger the sawteeth.

4. CONCLUSIONS

For two types of JET discharges it was shown that conditions are obtained in which ballooning modes may play an important role in the evolution of the discharge. In the high beta discharges, the plasma center is unstable to high-n ballooning modes. Because the unstable region is within the q = 1 surface, this instability probably does not have a large effect on the confinement properties as compared to the sawteeth. However, the ballooning instability could trigger the sawtooth.

In all the evaluated discharges with very large pressure gradients produced by pellet injection and additional heating, the discharges are marginally stable or unstable to ballooning modes. Although the stability boundary depends on the exact value of q_0, the cases analyzed show that the regions of the plasma with the large pressure gradients are unstable over the complete range within the error bars of the q_0 measurement. The driving force of these instabilities is the large pressure gradient region where the ballooning criterion is violated. This shows that the maximum achievable pressure gradient for the pellet discharges in JET is limited by the boundary of the first region of stability. The period of enhanced performance of the pellet discharge shown ends in a fast decay of β which is caused by an m/n = 3/2 mode. This is similar to the observations at the beta limit in Doublet DIII-D and TFTR , viz. violation of the ballooning criterion coincident with growth of an m/n = 3/2 or 2/1 mode. A possible way to avoid this limitation of the maximum pressure gradient would be to adjust the q profile in such a manner that the large gradients would lie in the second region of stability. Whether this is possible with the typical profiles of pellet discharges remains to be investigated.

Acknowledgements

We wish to acknowledge J.O'Rourke, G.Schmidt, J.A.Snipes, and the LIDAR team for their contribution of the diagnostic data. This work was supported by the "Nederlandse Organisatie voor Wetenschappelijk Onderzoek" (NWO) and by the Euratom association with the "Stichting voor Fundamenteel Onderzoek der Materie" (FOM).

References

BECKER G., ASDEX TEAM, NEUTRAL INJECTION TEAM (1987) Nucl. Fusion 27, 1785.
"Confinement and Ballooning Stability at the Beta Limit".

BLUM J., GILBERT J.C., LE FOLL J.,THOORIS B. (1986) 8th Europhysics Conf. on Computational Physics Computing in Plasma Physics, Eibsee , Vol. 10D,49.
"Numerical Identification of the Plasma Current Density in a Tokamak from the Experimental Measurements".

CONNOR J.W., HASTIE R.J., TAYLOR J.B. (1979) Proc. R. Soc. A365, 1.
"High Mode Number Stability of an Axisymmetric Toroidal Plasma".

GOEDBLOED J.P., HOGEWEY G.M.D., KLEIBERGEN R., REM J., GALVAO R.M.O., SAKANAKA P.H. (1984) Proc. 10th International IAEA Conf. on Plasma Physics and Controlled Nuclear Fusion Research, London, Vol. II, 165. IAEA, Vienna, 1985.
"Investigation of High-Beta Tokamak Stability with the Program HBT".

GRUBER O. et al. (1986) Proc. 11th International IAEA Conf. on Plasma Physics and Contr. Nucl. Fusion Research, Kyoto, 1986, Vol. I, 357. IAEA, Vienna, 1987.
"MHD Stability and Transport of Beam heated ASDEX Discharges in the Vicinity of the Beta Limit".

HASTIE R.J., TAYLOR J.B. (1981) Nucl. Fusion 21, 187.
"Validity of Ballooning Representation and Modenumber Dependence of Stability".

HENDER T.C., HAYNES P.S., ROBINSON D.C., SYKES A. (1987) 14th European Conf. on Controlled Fusion and Plasma Physics, Vol. I, 231.
"MHD Stability in JET with Peaked Pressure".

JET TEAM (1988) Proc. 12th International IAEA Conf. on Plasma Physics and Controlled Nuclear Fusion Research, Nice, IAEA-CN-50/A-IV-1.
"Heating of Peaked Density Profiles Produced by Pellet Injection in JET".

KAUFMAN M. et al. (1988) Nucl. Fusion 28, 827.
"Pellet Injection with Improved Confinement in ASDEX".

LAZZARO E., MANTICA P. (1988) Plasma Physics Contr. Fusion 30, 1735.
"Experimental Identification of Tokamak Equilibrium Using Magnetic and Diamagnetic Signals".

MANICKAM J., POMPHREY N., TODD A.M.M. (1987) Nucl. Fusion 27, 1461.
"Ideal MHD Stability Properties of Pressure Driven Modes in Low Shear Tokamaks".

MC GUIRE K.M. et al. (1988) Plasma Physics Contr. Fusion 30, 1391.
"Transport and Stability Studies on TFTR".

O'ROURKE J. et al. (1988) 15th European Conf. on Controlled Fusion and Plasma Heating, Dubrovnik, Vol. I, 155.
"Polarimetric Measurements of the q-profile".

SALZMANN H., HIRSCH K., NIELSEN P., GOWERS C., GADD A. GADEBERG M., MÜRMANN H., SCHRÖDTER C. (1987) Nucl. Fusion **27**, 1925
"First Results from the LIDAR Thomson Scattering System on JET"

SNIPES J.A., CAMPBELL D.J., HUGON M., MORGAN P., STORK D., SUMMER D., THOMSON K., TUBBING B. (1988) 15th European Conf. on Controlled Fusion and Plasma Physics, Dubrovnik, Vol.I, 346.
"Effects of Large Amplitude MHD Activity on Confinement in JET".

STRAIT E.J., LAO L., KELLMAN A.G., OSBORNE T.H., SNIDER R., STAMBAUGH R.D., TAYLOR T.S. (1989) Phys. Rev. Lett. **62**, 1282.
"MHD Instabilities near the Beta Limit in Doublet DIII-D Tokamak".

TROYON F., ROY A., COOPER W.A., YASSEEN F., TURNBULL A. (1988) Plasma Physics Contr. Fusion **30**, 1585.
"Beta Limits in Tokamaks. Experimental and Computational Status".

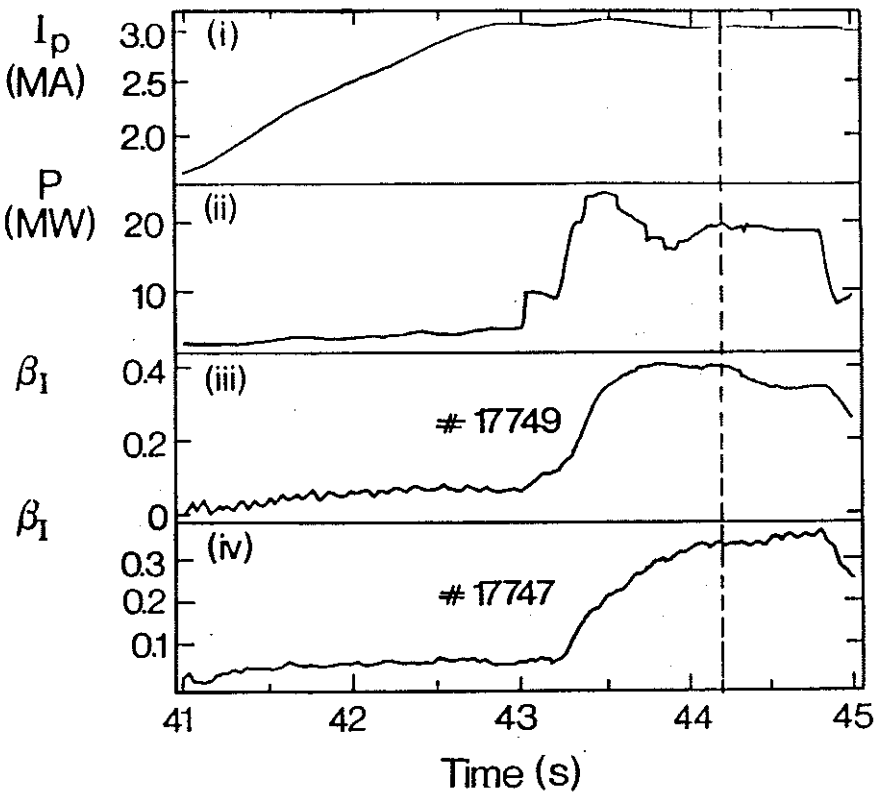

Fig. 1 Experimental data of pellet discharge #17749, i) plasmacurrent, ii) total heating power (Ohmic+NBI+ICRH), iii) poloidal beta of pellet discharge, pellet injected at t=42 sec, iv) poloidal beta of reference case shot #17747 without pellet injection.

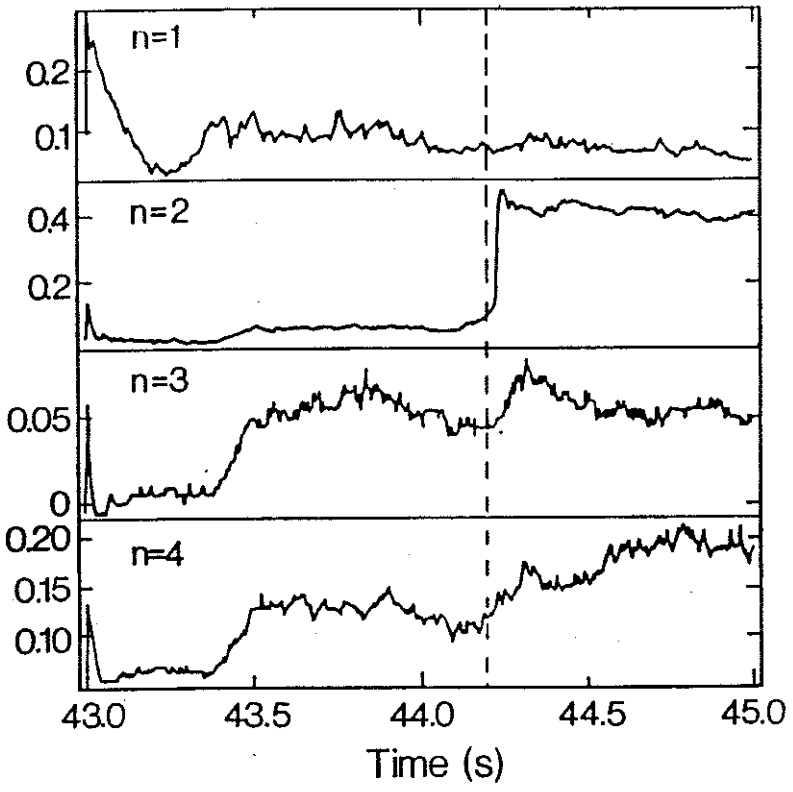

Fig. 2 MHD activity with toroidal modenumber i) $n=1$, ii) $n=2$, iii) $n=3$, iv) $n=4$ of pellet discharge #11749.

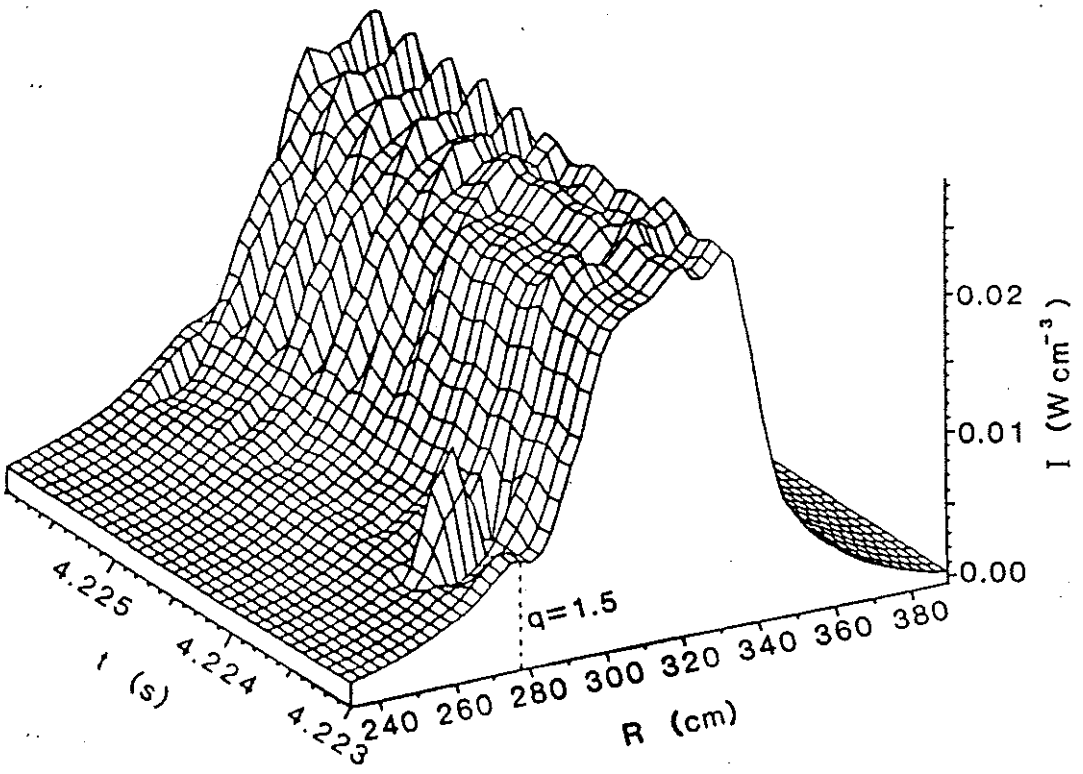

Fig. 3 Soft X-ray emission profile of the pellet discharge #17749 after the onset of the $n=2$ MHD activity.

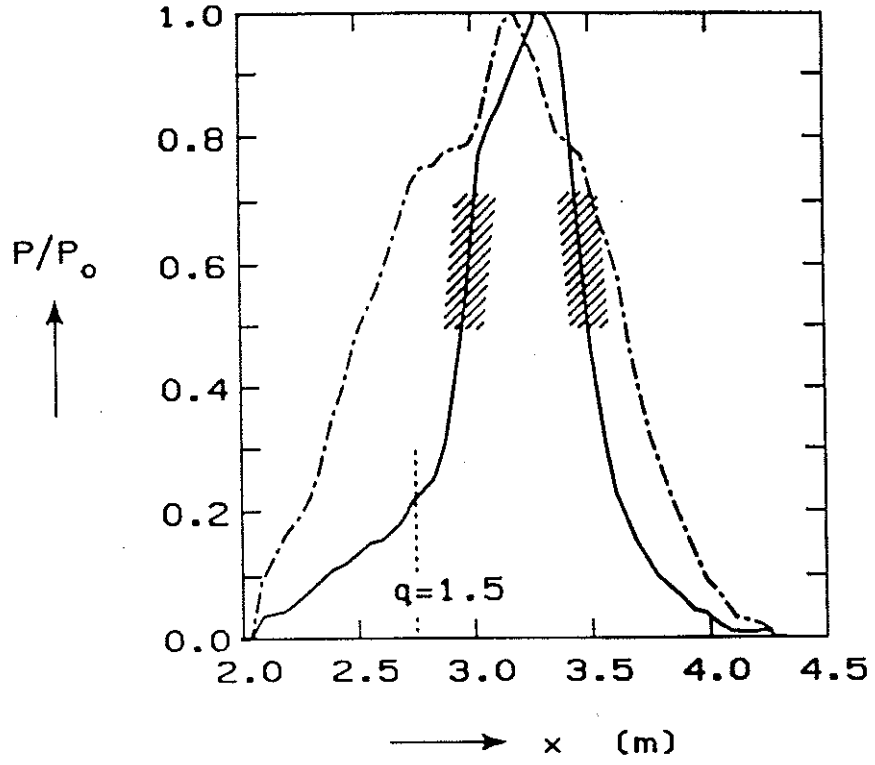

Fig. 4 The normalized electron pressure profiles from the LIDAR diagnostic of the pellet discharge #17749 (full curve) and a similar discharge without pellet injection shot #17747 (dashed curve). The maximum pressure are approximately 75 kPa for shot #17747 and 156 kPa for #17749. The unstable region is indicated by the shaded region.

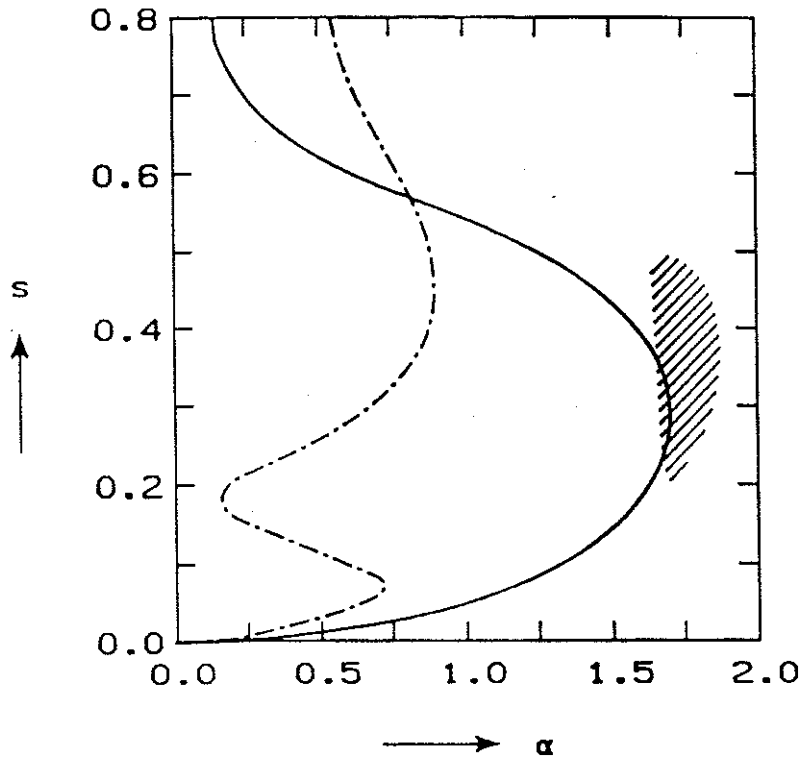

Fig. 5a The shear, $s=2(\psi/q)(dq/d\psi)$ versus the pressure gradient, $\alpha=-(4q^{*2}/\epsilon B^2)\sqrt{\psi}\, dp/d\psi$, of the pellet discharge #17749 (full curve) and of the reference discharge #17747 (dashed curve). The shaded area corresponds to the ballooning unstable region, i.e. the boundary of the first region of stability.

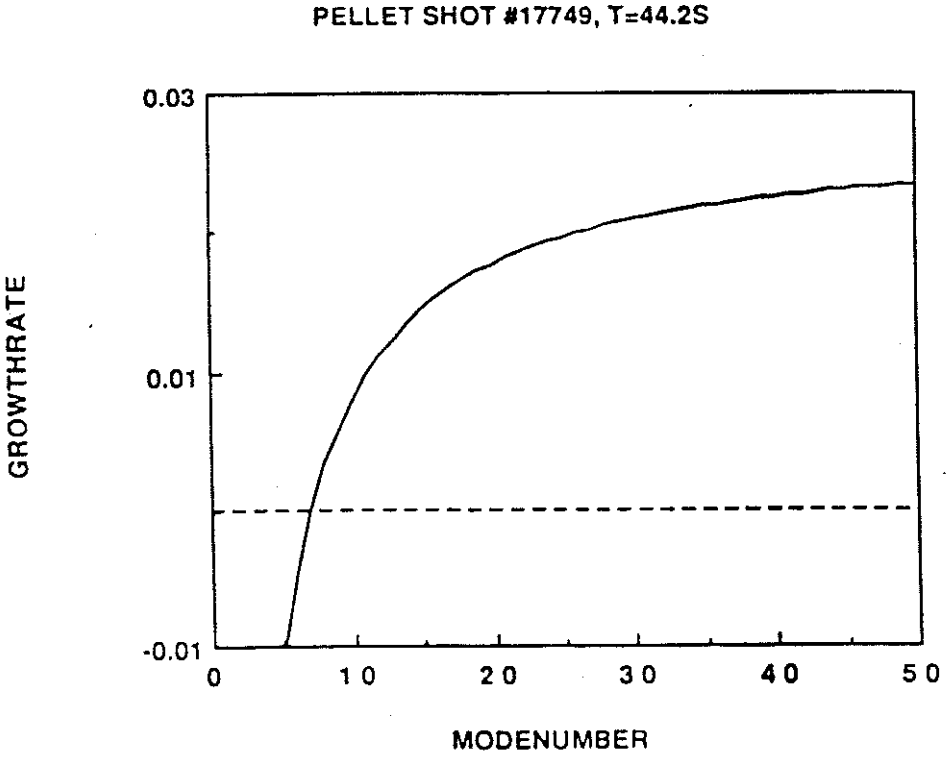

Fig. 5b The growth rate versus the toroidal modenumber of the ballooning instability at the largest pressure gradient of the pellet discharge.

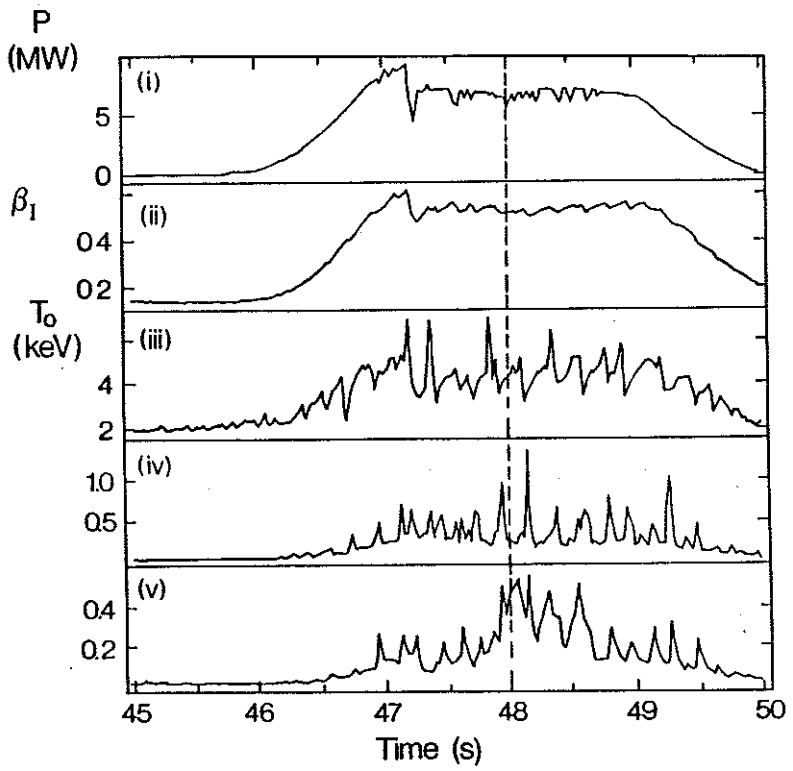

Fig. 6 Experimental data of the high beta discharge #14729; i) total RF power, ii) poloidal beta, iii) central electron temperature from electron cyclotron emission, iv) $n=1$ MHD activity, and v) $n=3$ MHD activity.

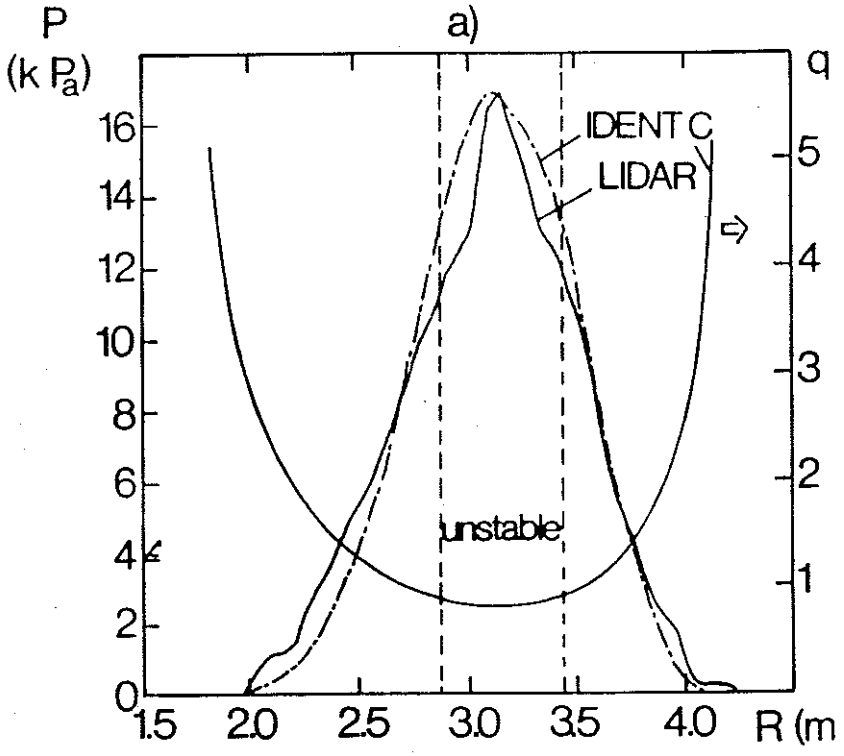

Fig. 7 The electron pressure profile measured by the LIDAR diagnostic system (full line) at $t=48$ sec and the corresponding normalized total pressure and q profiles determined by IDENTC for the high beta discharge #14729. The indicated region is unstable to ballooning modes.

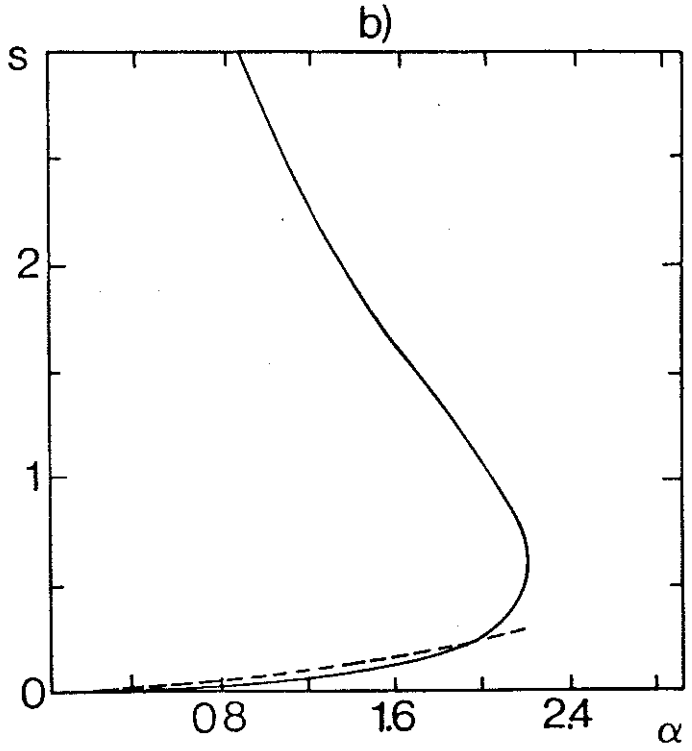

Fig. 8a The shear versus the pressure gradient diagram of the high beta discharge at $t=48$ sec. The unstable region is below the dashed curve which represents the boundary of the first region of stability.

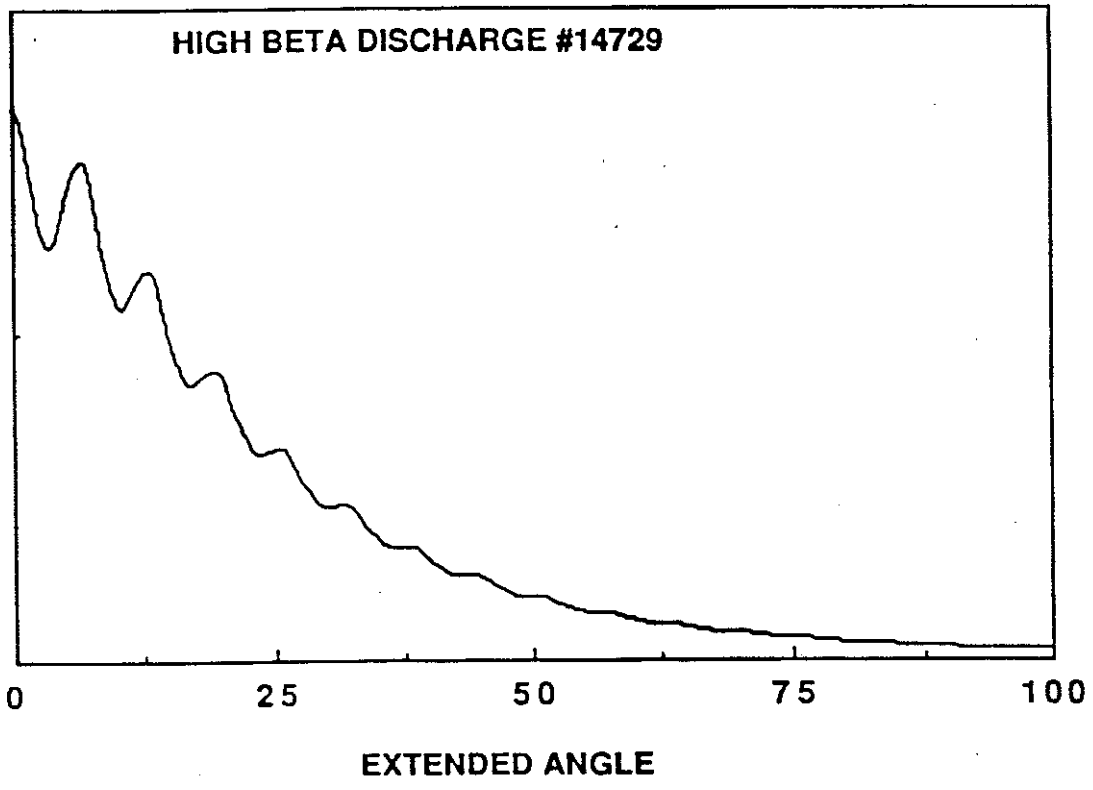

Fig. 8b The eigenfunction of the ballooning mode at the most unstable flux surface. Along the horizontal axis the extended poloidal angle is plotted. The eigenfunction is symmetric with respect to $\theta=0$.

APPENDIX 1.

THE JET TEAM

JET Joint Undertaking, Abingdon, Oxon, OX14 3EA, U.K.

J.M.Adams[1], F.Alladio[4], H.Altmann, R.J.Anderson, G.Appruzzese, W.Bailey, B.Balet, D.V.Bartlett, L.R.Baylor[24], K.Behringer, A.C.Bell, P.Bertoldi, E.Bertolini, V.Bhatnagar, R.J.Bickerton, A.Boileau[3], T.Bonicelli, S.J.Booth, G.Bosia, M.Botman, D.Boyd[31], H.Brelen, H.Brinkschulte, M.Brusati, T.Budd, M.Bures, T.Businaro[4], H.Buttgereit, D.Cacaut, C.Caldwell-Nichols, D.J.Campbell, P.Card, J.Carwardine, G.Celentano, P.Chabert[27], C.D.Challis, A.Cheetham, J.Christiansen, C.Christodoulopoulos, P.Chuilon, R.Claesen, S.Clement[30], J.P.Coad, P.Colestock[6], S.Conroy[13], M.Cooke, S.Cooper, J.G.Cordey, W.Core, S.Corti, A.E.Costley, G.Cottrell, M.Cox[7], P.Cripwell[13], F.Crisanti[4], D.Cross, H.de Blank[16], J.de Haas[16], L.de Kock, E.Deksnis, G.B.Denne, G.Deschamps, G.Devillars, K.J.Dietz, J.Dobbing, S.E.Dorling, P.G.Doyle, D.F.Düchs, H.Duquenoy, A.Edwards, J.Ehrenberg[14], T.Elevant[12], W.Engelhardt, S.K.Erents[7], L.G.Eriksonn[5], M.Evrard[2], H.Falter, D.Flory, M.Forrest[7], C.Froger, K.Fullard, M.Gadeberg[11], A.Galetsas, R.Galvao[8], A.Gibson, R.D.Gill, A.Gondhalekar, C.Gordon, G.Gorini, C.Gormezano, N.A.Gottardi, C.Gowers, B.J.Green, F.S.Griph, M.Gryzinski[26], R.Haange, G.Hammett[6], W.Han[9], C.J.Hancock, P.J.Harbour, N.C.Hawkes[7], P.Haynes[7], T.Hellsten, J.L.Hemmerich, R.Hemsworth, R.F.Herzog, K.Hirsch[14], J.Hoekzema, W.A.Houlberg[24], J.How, M.Huart, A.Hubbard, T.P.Hughes[32], M.Hugon, M.Huguet, J.Jacquinot, O.N.Jarvis, T.C.Jernigan[24], E.Joffrin, E.M.Jones, L.P.D.F.Jones, T.T.C.Jones, J.Källne, A.Kaye, B.E.Keen, M.Keilhacker, G.J.Kelly, A.Khare[15], S.Knowlton, A.Konstantellos, M.Kovanen[21], P.Kupschus, P.Lallia, J.R.Last, L.Lauro-Taroni, M.Laux[33], K.Lawson[7], E.Lazzaro, M.Lennholm, X.Litaudon, P.Lomas, M.Lorentz-Gottardi[2], C.Lowry, G.Magyar, D.Maisonnier, M.Malacarne, V.Marchese, P.Massmann, L.McCarthy[28], G.McCracken[7], P.Mendonca, P.Meriguet, P.Micozzi[4], S.F.Mills, P.Millward, S.L.Milora[24], A.Moissonnier, P.L.Mondino, D.Moreau[17], P.Morgan, H.Morsi[14], G.Murphy, M.F.Nave, M.Newman, L.Nickesson, P.Nielsen, P.Noll, W.Obert, D.O'Brien, J.O'Rourke, M.G.Pacco-Düchs, M.Pain, S.Papastergiou, D.Pasini[20], M.Paume[27], N.Peacock[7], D.Pearson[13], F.Pegoraro, M.Pick, S.Pitcher[7], J.Plancoulaine, J-P.Poffé, F.Porcelli, R.Prentice, T.Raimondi, J.Ramette[17], J.M.Rax[27], C.Raymond, P-H.Rebut, J.Removille, F.Rimini, D.Robinson[7], A.Rolfe, R.T.Ross, L.Rossi, G.Rupprecht[14], R.Rushton, P.Rutter, H.C.Sack, G.Sadler, N.Salmon[13], H.Salzmann[14], A.Santagiustina, D.Schissel[25], P.H.Schild, M.Schmid, G.Schmidt[6], R.L.Shaw, A.Sibley, R.Simonini, J.Sips[16], P.Smeulders, J.Snipes, S.Sommers, L.Sonnerup, K.Sonnenberg, M.Stamp, P.Stangeby[19], D.Start, C.A.Steed, D.Stork, P.E.Stott, T.E.Stringer, D.Stubberfield, T.Sugie[18], D.Summers, H.Summers[20], J.Taboda-Duarte[22], J.Tagle[30], H.Tamnen, A.Tanga, A.Taroni, C.Tebaldi[23], A.Tesini, P.R.Thomas, E.Thompson, K.Thomsen[11], P.Trevalion, M.Tschudin, B.Tubbing, K.Uchino[29], E.Usselmann, H.van der Beken, M.von Hellermann, T.Wade, C.Walker, B.A.Wallander, M.Walravens, K.Walter, D.Ward, M.L.Watkins, J.Wesson, D.H.Wheeler, J.Wilks, U.Willen[12], D.Wilson, T.Winkel, C.Woodward, M.Wykes, I.D.Young, L.Zannelli, M.Zarnstorff[6], D.Zasche[14], J.W.Zwart.

PERMANENT ADDRESS

1. UKAEA, Harwell, Oxon. UK.
2. EUR-EB Association, LPP-ERM/KMS, B-1040 Brussels, Belgium.
3. Institute National des Récherches Scientifique, Quebec, Canada.
4. ENEA-CENTRO Di Frascati, I-00044 Frascati, Roma, Italy.
5. Chalmers University of Technology, Göteborg, Sweden.
6. Princeton Plasma Physics Laboratory, New Jersey, USA.
7. UKAEA Culham Laboratory, Abingdon, Oxon. UK.
8. Plasma Physics Laboratory, Space Research Institute, Sao José dos Campos, Brazil.
9. Institute of Mathematics, University of Oxford, UK.
10. CRPP/EPFL, 21 Avenue des Bains, CH-1007 Lausanne, Switzerland.
11. Risø National Laboratory, DK-4000 Roskilde, Denmark.
12. Swedish Energy Research Commission, S-10072 Stockholm, Sweden.
13. Imperial College of Science and Technology, University of London, UK.
14. Max Planck Institut für Plasmaphysik, D-8046 Garching bei München, FRG.
15. Institute for Plasma Research, Gandhinagar Bhat Gujat, India.
16. FOM Instituut voor Plasmafysica, 3430 Be Nieuwegein, The Netherlands.
17. Commissiariat à L'Energie Atomique, F-92260 Fontenay-aux-Roses, France.
18. JAERI, Tokai Research Establishment, Tokai-Mura, Naka-Gun, Japan.
19. Institute for Aerospace Studies, University of Toronto, Downsview, Ontario, Canada.
20. University of Strathclyde, Glasgow, G4 ONG, U.K.
21. Nuclear Engineering Laboratory, Lapeenranta University, Finland.
22. JNICT, Lisboa, Portugal.
23. Department of Mathematics, Univeristy of Bologna, Italy.
24. Oak Ridge National Laboratory, Oak Ridge, Tenn., USA.
25. G.A. Technologies, San Diego, California, USA.
26. Institute for Nuclear Studies, Swierk, Poland.
27. Commissiariat à l'Energie Atomique, Cadarache, France.
28. School of Physical Sciences, Flinders University of South Australia, South Australia SO42.
29. Kyushi University, Kasagu Fukuoka, Japan.
30. Centro de Investigaciones Energeticas Medioambientales y Techalogicas, Spain.
31. University of Maryland, College Park, Maryland, USA.
32. University of Essex, Colchester, UK.
33. Akademie de Wissenschaften, Berlin, DDR.

CR 88.49.1A